

EFFECTS OF NEUTRINO ELECTROMAGNETIC FORM FACTORS ON NEUTRINO INTERACTION WITH FINITE TEMPERATURE ELECTRON MATTERS

Listiana Satiawati^{*)} and Anto Sulaksono

Department of Physics, Faculty of Mathematic and Natural Sciences, Universitas Indonesia, Depok 16424, Indonesia

^{*)}E-mail: listianasatiawati@yahoo.com

Abstract

The differential cross-section of neutrino interaction with dense and warm electron gases has been calculated by taking into account the neutrino electromagnetic form factors. The significant effect of electromagnetic properties of neutrino can be found if the neutrino dipole moment, μ_ν , is $\geq 5.10^{-9} \mu_B$ and neutrino charge radius, R_ν , is $\geq 5.10^{-6} \text{ MeV}^{-1}$. The importance of the retarded correction, detailed balance and Pauli blocking factors is shown and analyzed. Many-body effects on the target matter which are included via random phase approximation (RPA) correlation as well as photon effective mass are also investigated.

Keywords: neutrino, supernova atmosphere, temperature and matter effects

1. Introduction

The neutrino interaction in hot and dense matters is very important tools to study the behavior of the neutron star and supernova, because neutrino is the most accurate information messenger about the state in the core of the star (see Refs. [1-2] and references therein). According to the standard model of particle physics, neutrinos are neutral particles and have no mass. They interact with other particles only through weak interaction. But in fact, the experimental observations and the observations from terrestrial sources indicate that neutrino has indeed a small mass, i.e. smaller than 5.7 eV [3]. Neutrino has also a dipole moment [4] and charge radius [5]. These facts indicate that neutrinos can interact with other particles not only through weak interaction, but also through electromagnetic interaction.

The neutrino differential cross section and mean free path in matters calculations by taking into account the electromagnetic form factor correction for matter consist of a variety of constituents in the zero temperature approximation has been studied previously in Refs. [6-7]. The results have been developed in this work for special case, i.e. for electron gasses by generalizing the calculation into finite temperature situation. It is worth note-taking that, for the case of finite temperature, the correlations among the target electrons within the random phase approach (RPA) framework are needed to be taken into account. Effect of the effective mass of the photon in the medium should

be also considered. Retardation factor should be added to the tensor polarization of the target particle. Pauli blocking effect which limits the possibility of the outgoing particle states should be also considered. The latter effect is known to significantly decrease the differential cross-section of neutrinos [1]. Based on the fluctuation-dissipation theorem which requires the interaction should be invariant in respect to the inversion of space, the detailed balance factor is also needed to be taken into account [8-10]. These mentioned effects together with the effects of neutrinos electromagnetic form factors are the main focus of this investigation.

This paper is organized as follows: In Sec. 2, the analytical results of the scattering cross-section neutrino interaction with electrons gas are given. Sec. 3 contains the discussions of the results from numerical calculations while the conclusion is given in Sec. 4.

2. Methods

In this section brief explanations of the neutrino electromagnetic form factors, the cross-section of neutrino interactions with electron in vacuum as an illustration before entering into the cross-section of neutrino interactions with electron in the electron matters as well as the cross-section of neutrino interactions with electron in the electron matters calculation itself, are given.

Neutrino electromagnetic form factors. Although neutrino is a neutral particle, but we can assumed that neutrino is not a point particle so that it can have a charge distribution. Therefore, as the further consequence, the neutrino form factors are not equal to zero for $q \neq 0$ [11-12]. Matrix elements of electromagnetic current between the initial state ν_i with momentum k_i and the final state ν_j with momentum k_j of Dirac neutrinos is,

$$\langle \nu_j^D(k_j) | J_\mu^{EM} | \nu_i^D(k_i) \rangle = \bar{u}(k') [f_{1\nu} \gamma^\mu + g_{1\nu} \gamma^\mu \gamma^5 - (f_{2\nu} + i g_{2\nu} \gamma^5) \frac{P^\mu}{2m_e}] u(k), \quad (1)$$

where $k' = k + q$, $P^\mu = k^\mu + k'^\mu = 2k^\mu - q^\mu$.

$f_{1\nu}$, $g_{1\nu}$, $f_{2\nu}$ and $g_{2\nu}$ are the Dirac, anapole, magnetic and electric form factors respectively [5,13], and q is momentum transfer.

The average of neutrino charge radius is given by the second term of the expansion in the Dirac and anapole neutrino form factor $f(q^2)$ in respect to q^2 [11-12]. For the Dirac form factor, the squared vector charge radius of neutrino is $\langle r_v^2 \rangle = -6f_{1\nu}(0)$, while for the anapole form factor, the squared axial-vector charge radius of neutrino is $\langle r_A^2 \rangle = -6g_{1\nu}(0)$. Thus,

$$f_{1\nu}^2 + g_{1\nu}^2 = \frac{1}{36} (a^4 + b^4) q^4 = \frac{1}{36} R^4 q^4, \quad (2)$$

R is a quantity that can be observed experimentally.

According to Ref. [11-12], the charge radius of neutrino predicted from Kamiokande solar neutrino analysis is $\langle R^2 \rangle = 10^{-34} \text{ cm}^2$. If it is converted to $1 \text{ cm} = 5.07 \times 10^{10} \text{ MeV}^{-1}$, the obtained $R \approx 10^{-6} \text{ MeV}^{-1}$. The magnetic and electric form factors for $q^2 = 0$ give the static moments (diagonal) of neutrinos in units of Bohr magneton ($\mu_B = e/2m_e$). The static magnetic dipole moment is $m_v = f_{2\nu}(0) \mu_B$, and the static electric dipole moment is $d_v = g_{2\nu}(0) \mu_B$,

$$f_{2\nu}^2(0) + g_{2\nu}^2(0) = \left(\frac{m_v}{\mu_B} \right)^2 + \left(\frac{d_v}{\mu_B} \right)^2 \equiv \frac{\mu_v^2}{\mu_B^2},$$

$$\mu_v = [f_{2\nu}^2(0) + g_{2\nu}^2(0)]^{1/2} \mu_B \quad (3)$$

According to Ref. [14-15], the dipole moment of the electron neutrino predicted from analysis of some experimental results is around $\mu_v \approx 10^{-10} \mu_B$.

Scattering of neutrino with electron in a vacuum condition. The relevant Lagrangian interaction of the Weinberg-Salam theory on the state with momentum-transfer which is much smaller than the mass of the weak gauge bosons can be represented in the form of effective contact of four-point interactions. So the

Lagrangian density for neutrino-electron interaction of neutral current (Z^0), charged current (W^\pm) and electromagnetic current contributions can be comprehensively written as,

$$L_{\text{int}} = \frac{G_F}{\sqrt{2}} \bar{u}(k') \Gamma_w^\mu u(k) \bar{u}(p') J_\mu^w u(p) + \frac{4\pi\alpha}{q^2} \bar{u}(k') \Gamma_{EM}^\mu u(k) \bar{u}(p') J_\mu^{EM} u(p) \quad (4)$$

$u(k)$ and $u(p)$ are the spinor of neutrino and electron, while Γ and J are the electron and neutrino currents. Here, $C_V = 2 \sin^2 \theta_W + 1/2$ is the vector coupling constant, $C_A = 1/2$ is the axial coupling constant, θ_W is the Weinberg angle ($\sin^2 \theta_W \equiv 0.223$), while $G_F = 1.66 \times 10^{-11} \text{ MeV}^{-2}$ is the weak interaction coupling constant, and $\alpha = e^2/4\pi \cong 1/137$ is the electromagnetic fine structure constant. Transition matrix for the weak interaction of Eq. (4) is [16]

$$M_w = \frac{G_F}{\sqrt{2}} [\bar{u}(k') \gamma^\mu (1 + \gamma^5) u(k)] \times [\bar{u}(p') \gamma_\mu (C_V + C_A \gamma^5) u(p)], \quad (5)$$

Vertex form $\gamma^\mu (1 + \gamma^5)$ means a violation to conservation of parity term is present. While the transition matrix for the electromagnetic interaction is

$$M_{EM} = \frac{4\pi\alpha}{q^2} [\bar{u}(p') \gamma_\mu u(p)] \{ \bar{u}(k') [f_{1\nu} \gamma^\mu + g_{1\nu} \gamma^\mu \gamma^5 - (f_{2\nu} + i g_{2\nu} \gamma^5) \frac{P^\mu}{2m_e}] u(k) \} \quad (6)$$

The above transition matrices contain information of the interaction in the scattering process. The square of the transition matrix (M^2) is the interaction probability to obtain a final state after the passage of the projectile particle hits targets during interaction process. The probability of interaction is proportional to the differential cross-section ($d\sigma \propto M^2$). Since the transition matrix of the total neutrino-electron interaction is $M_{\text{Total}} = M_w + M_{EM}$ then the differential cross-section can be written [6],

$$d\sigma \propto M^2 \propto \left(\frac{G_F}{\sqrt{2}} \right)^2 L_{\mu\nu}^{(W)} L_{\nu\mu}^{\mu\nu(W)} + \left(\frac{4\pi\alpha}{q^2} \right)^2 L_{\mu\nu}^{(EM)} L_{\nu\mu}^{\mu\nu(EM)} + \frac{8G_F \pi\alpha}{q^2 \sqrt{2}} L_{\mu\nu}^{(INT)} L_{\nu\mu}^{\mu\nu(INT)}, \quad (7)$$

The contribution of weak interactions is

$$L_{\mu\nu}^{(W)} = C_V^2 \text{Tr}[(\not{p}' + m_e) \gamma_\mu (\not{p} + m_e) \gamma_\nu] + 2C_V C_A \text{Tr}[(\not{p}' + m_e) \gamma_\mu (\not{p} + m_e) \gamma_\nu \gamma^5] + 2C_A^2 \text{Tr}[(\not{p}' + m_e) \gamma_\mu \gamma^5 (\not{p} + m_e) \gamma_\nu \gamma^5], \quad (8)$$

for the electron current, and

$$L_v^{\mu\nu(W)} = Tr[\mathbf{k}'\gamma^\mu(1+\gamma^5)\mathbf{k}\gamma^\nu(1+\gamma^5)], \quad (9)$$

for the neutrino current. The electromagnetic contribution is

$$L_{\mu\nu}^{(EM)} = Tr[(\mathbf{p}'+m_e)\gamma_\mu(\mathbf{p}+m_e)\gamma_\nu] \quad (10)$$

for the electron current, and

$$\begin{aligned} L_v^{\mu\nu(EM)} = Tr\{ & \mathbf{k}'[f_{1\nu}\gamma^\mu + g_{1\nu}\gamma^\mu\gamma^5 \\ & - (f_{2\nu} + ig_{2\nu}\gamma^5)\frac{P^\mu}{2m_e}]\mathbf{k}[f_{1\nu}\gamma^\nu + g_{1\nu}\gamma^\nu\gamma^5 \\ & - (f_{2\nu} + ig_{2\nu}\gamma^5)\frac{P^\nu}{2m_e}]\} \end{aligned} \quad (11)$$

for the neutrino current. The interference contribution is

$$\begin{aligned} L_{\mu\nu}^{(INT)} = C_V Tr[(\mathbf{p}'+m_e)\gamma_\mu + (\mathbf{p}+m_e)\gamma_\nu] \\ + C_A Tr[(\mathbf{p}'+m_e)\gamma_\mu\gamma^5 + (\mathbf{p}+m_e)\gamma_\nu] \end{aligned} \quad (12)$$

for the electron current, and

$$\begin{aligned} L_v^{\mu\nu(INT)} = Tr[\mathbf{k}'\gamma^\mu(1+\gamma^5)\mathbf{k}[f_{1\nu}\gamma^\mu + g_{1\nu}\gamma^\mu\gamma^5 \\ - (f_{2\nu} + ig_{2\nu}\gamma^5)\frac{P^\mu}{2m_e}]] \end{aligned} \quad (13)$$

for the neutrino current, \mathbf{k} and \mathbf{p} in Eqs. (8) – (13) is $k^\mu\gamma_\mu$ and $p^\mu\gamma_\mu$ respectively.

Scattering of neutrino with electrons in a medium. In a medium, a quite number of electrons are involved so that the $L_{\mu\nu}$ current should be modified by medium effects [17]. In this case, the electron current used in vacuum replaces by the electronic polarization tensor ($\Pi_{\mu\nu}^I$), $L_{\mu\nu} \rightarrow \Pi_{\mu\nu}^I$. The explicit form of polarization tensor will be discussed in this section. Index I here means an imaginary component. In scattering of neutrinos with the electron gasses, electron gasses should be considered as a many-body system. Collision of neutrino with one target-electron of the electron gasses, cause an interaction-between the target-electron with surrounding electrons. The sum of all possible circumstances of such interaction is taken into account in polarizations. Generalization of Eq. (7) for the differential cross-section equation of neutrino-electron scattering in dense medium at finite temperature, with the addition of several correction factors and correlations can be calculated. The explicit form of the differential cross-section equation is [16],

$$\frac{1}{V} \frac{d^3\sigma}{d^2\Omega dE'_\nu} = -\frac{1}{16\pi^2} \frac{E'_\nu}{E_\nu} \left[\left(\frac{G_F}{\sqrt{2}} \right)^2 L_v^{\mu\nu(W)} \Pi_{\mu\nu}^{ImR(W)} \right.$$

$$\begin{aligned} & + \left(\frac{4\pi\alpha}{(q_\mu^2)'} \right)^2 L_v^{\mu\nu(EM)} \Pi_{\mu\nu}^{ImR(EM)} \\ & + \frac{8G_F\pi\alpha}{(q_\mu^2)'\sqrt{2}} L_v^{\mu\nu(INT)} \Pi_{\mu\nu}^{ImR(INT)}] \\ & \times dbf \times Pbf. \end{aligned} \quad (14)$$

With E_ν and E'_ν is the neutrino energy before and after scattering, μ_ν is neutrino chemical potential, T is temperature and q_0 and q_μ is energy and four momentum transfer, $\Pi_{\alpha\beta}^{ImR} = \tanh(q_0/2T)$, $\Pi_{\alpha\beta}^{Im}$ is retardation factor [8-9], $dbf = [1 - \exp(-q_0/T)]^{-1}$ is the detailed balance factor [8] and $Pbf = 1 - \{1 + \exp[(E_\nu + q_0 + \mu_\nu)/T]\}^{-1}$ is the Pauli blocking factor [8]. These three factors above should be included for finite temperature calculation. And in many-body calculation, RPA correlations and photon effective mass is also taken into account.

The effective photon mass correction is [18],

$$(q_\mu^2)' = q_\mu^2 + m_i^2(T, \rho_e), \quad (15)$$

where m_i^2 is the effective photon mass [19],

$$m_i^2 = \frac{4\alpha}{\pi} \int_0^\infty dp \frac{p^2}{E} [f_+(E) + f_-(E)], \quad (16)$$

where $f_\pm(E) = [1 + \exp(E \mp \beta\alpha)]^{-1}$. In addition to the photon effective mass, the effect of anti-particle factor ($f_-(E)$) is also significant in this polarization because the particle target in this paper, i.e. an electron, has a quite small mass. Anti-particle effects on the polarization can be seen more clearly later in Eq. (23).

A common form of the tensor polarization of the electron gasses ($\Pi_{\mu\nu}$) from Eq. (14) is

$$\begin{aligned} \Pi_{\mu\nu}^{Im} = & -\frac{1}{(2\pi)^2} \int \frac{d^3p}{8E_p E_{p+q}} f(E_p) [1 - f(E_{p+q})] \\ & \times F_{\mu\nu}(p, p+q) \{ \delta[q_0 - (E_{p+q} - E_p)] \\ & + \delta[q_0 - (E_p - E_{p+q})] \}. \end{aligned} \quad (17)$$

Polarization can be divided into 3 parts, the first is vector polarization ($\sim F_{\mu\nu}^V$), the second is vector-axial polarization ($\sim F_{\mu\nu}^{VA}$) and the third is axial polarization ($\sim F_{\mu\nu}^A$).

Vector polarization consists of two components which are not mutually dependent, i.e. longitudinal polarization (Π_L) and transverse polarization (Π_T) [16]. While the vector-axial section produces vector-axial polarization (Π_{VA}) and the axial section produces axial polarization (Π_A). Furthermore, the components of

polarization tensor of electron gasses above can be derived from Eq. (17), the result is [16]

$$\Pi_T' = \frac{q_\mu^2}{4\pi |\vec{q}|^3} \int_{e_-}^{\infty} dE_p [(E_p + \frac{1}{2}q_0)^2 + \frac{1}{4}|\vec{q}|^2 + \frac{m_e^2 |\vec{q}|^2}{q_\mu^2}] \times [F(E_p, E_p + q_0) + F(E_p + q_0, E_p)]. \quad (18)$$

$$\Pi_L' = \frac{q_\mu^2}{2\pi |\vec{q}|^3} \int_{e_-}^{\infty} dE_p [(E_p + \frac{1}{2}q_0)^2 - \frac{1}{4}|\vec{q}|^2] \times [F(E_p, E_p + q_0) + F(E_p + q_0, E_p)]. \quad (19)$$

$$\Pi_A' = \frac{m_e^2}{(2\pi)^2} \int_{e_-}^{\infty} dE_p \times [F(E_p, E_p + q_0) + F(E_p + q_0, E_p)]. \quad (20)$$

$$\Pi_{VA}' = \frac{q_\mu^2}{8\pi |\vec{q}|^3} \int_{e_-}^{\infty} dE_p (2E_p + q_0) \times [F(E_p, E_p + q_0) + F(E_p + q_0, E_p)]. \quad (21)$$

$$\text{where } e_- = -\frac{1}{2}q_0 + \frac{1}{2}|\vec{q}| \sqrt{1 - \frac{4m_e^2}{q_\mu^2}},$$

e_- is the kinematic constraints. Because neutrinos and electrons are fermions, then the Fermi-Dirac distribution is used. For the sake of convenience, we define $F(E, E^*)$ in Eqs. (19)–(20) [10,20]

$$F(E, E^*) \equiv f_+(E)(1 - f_+(E^*)) + sf_-(E)(1 - f_-(E^*)),$$

$s=1$ for the longitudinal, transverse and axial polarization and -1 for the vector-axial polarization. We can also write

$$F(E, E + q_0) + F(E + q_0, E) = F_+(E, q_0) + sF_-(E + q_0, q_0) \quad (22)$$

where

$$F_+(E, q_0) = \frac{e^{E\beta - \alpha}(1 + e^{\beta q_0})}{(1 + e^{E\beta - \alpha})(1 + e^{(E+q_0)\beta - \alpha})},$$

$$F_-(E + q_0, q_0) = \frac{e^{E\beta + \alpha}(1 + e^{\beta q_0})}{(1 + e^{E\beta + \alpha})(1 + e^{(E+q_0)\beta + \alpha})}. \quad (23)$$

Physical meaning of the equation $F(E, E+q_0)+F(E+q_0, E)$ appears more clearly if it is written in the form of Eq. (23), where F_+ is the particle contribution while F_- is anti-particle contribution. Eqs. (18)–(21) agrees with the results found in Refs. [8-10].

The form of neutrino tensors in medium is the same as the one in vacuum, in which they also do not depend on temperature. Explicit forms of the tensor of neutrinos for weak interaction, electromagnetic interaction and interference in Eqs. (9), (11) and (13) can be seen in Ref. [16].

The product of neutrino and electron tensors can be used to determine contraction of each pair tensors in Eq. (14), where the explicit forms are derived in Ref. [16]. Here we only show the final results. Contraction for weak interaction, consisting of contraction of the vector, axial and axial-vector

$$L_\nu^{\mu\nu} \Pi_{\mu\nu}^{\text{Im}(W)} = -8q_\mu^2 (A_W R_{W_1} + R_{W_2} + R_{W_3} B_W), \quad (24)$$

where

$$A_W = \frac{2E(E - q_0) + \frac{1}{2}q_\mu^2}{|\vec{q}|^2}, \quad B_W = 2E - q_0,$$

$$R_{W_1} = (C_V^2 + C_A^2)(\Pi_L + \Pi_T),$$

$$R_{W_2} = C_V^2 \Pi_T + C_A^2 (\Pi_T - \Pi_A) \text{ and}$$

$$R_{W_3} = 2C_V C_A \Pi_{VA}.$$

Contraction for electromagnetic interaction, only consists of the vector

$$L_\nu^{\mu\nu} \Pi_{\mu\nu}^{\text{Im}(EM)} = A_{EM} R_{EM_1} - B_{EM} R_{EM_2}, \quad (25)$$

where

$$a = 4(f_{1\nu}^2 + g_{1\nu}^2), \quad b = \frac{f_{2\nu}^2 + g_{2\nu}^2}{m_e^2},$$

$$A_{EM} = [(bq_\mu^2 - a)A_W + \frac{1}{2}bq_\mu^2]q_\mu^2,$$

$$B_{EM} = (\frac{1}{2}bq_\mu^2 + a)q_\mu^2, \quad R_{EM_1} = \Pi_L + \Pi_T$$

$$\text{and } R_{EM_2} = \Pi_T.$$

$f_{1\nu}^2 + g_{1\nu}^2$ is the square of neutrino charge radius, and $f_{2\nu}^2 + g_{2\nu}^2$ is the square of neutrino dipole moment.

Contraction for interference, consisting of contraction of the vector and axial-vector

$$L_\nu^{\mu\nu} \Pi_{\mu\nu}^{\text{Im}(INT)} = -4\tilde{a}q_\mu^2 (A_{INT} R_{INT_1} + R_{INT_2} + B_{INT} R_{INT_3}), \quad (26)$$

where

$$\tilde{a} = f_{1\nu} + g_{1\nu}, \quad A_{INT} = A_W, \quad B_{INT} = B_W,$$

$$R_{INT_1} = C_V (\Pi_L + \Pi_T), \quad R_{INT_2} = C_V \Pi_T$$

$$\text{and } R_{INT_3} = C_A \Pi_{VA}.$$

RPA polarizations propagator expressed as a sum of several Feynman diagrams. These diagrams are a set of all ring diagrams, where the particle-hole excitations are automatically taken into account [17]. Explicit form of RPA correlations on the polarization can be obtained by solving the Dyson equation, the explicit expression can be found in Ref. [16].

Explicit forms of real and imaginary components of polarization for zero temperature can be obtained in Refs. [21- 22], and the real polarization components for finite temperatures can be found in Ref. [9], and for imaginary component, they are already shown in Eqs.

(19)-(21). This is the main analytical results of this work. In the following sections, the numerical results and discussion will be given.

3. Results and Discussion

In this section, first, the polarizations and cross-section will be discussed for the case of an electron in medium that are not correlated (linear response approach) in detail. After that, the analysis of the RPA correlation effects on electron medium, as well as the effective photon mass effects in the medium will be given.

Linear response approach. To find out what factors that control the behavior of the cross-section of neutrino scattering by electrons, the influence of variations in energy transfer (q_0) with different temperatures at fixed electron density of the four imaginary parts of polarization Π'_L , Π'_T , Π'_A and Π'_{VA} was studied. The results are shown in Fig. 1. In the longitudinal (Π_L) and transverse (Π_T) polarizations, it is obvious that the values of both polarizations increase with increasing temperature. But in the case of vector-axial polarization (Π_{VA}) the situation is opposite, in which with increasing temperature the value of polarization is decrease. The axial polarization (Π_A) is not sensitive to temperature changes. However the dominant contributions of the polarizations on the cross-section come from transverse and longitudinal polarizations. So it can be concluded that the cross-section is mainly determined by the behavior of the longitudinal and transverse polarizations

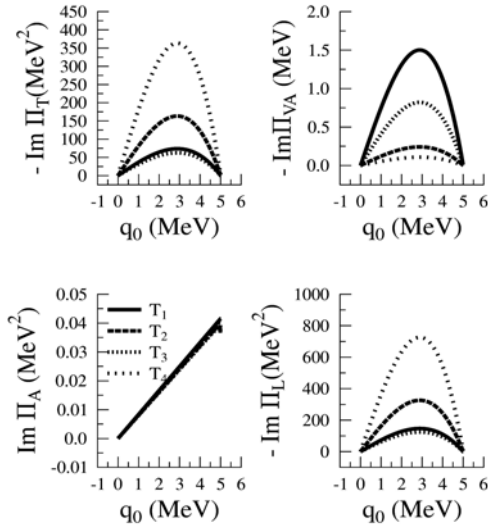


Figure 1. Comparison of Longitudinal (Π_L), Transverse (Π_T), Axial (Π_A), and Vector-axial Polarization (Π_{VA}) for Fixed Electron Density but with Temperature Variation ($T_1 = 0$ MeV, $\mu_1 = 50$ MeV, $T_2 = 20$ MeV, $\mu_2 = 26.79$ MeV, $T_3 = 40$ MeV, $\mu_3 = 7.88$ MeV, $T_4 = 60$ MeV, $\mu_4 = 3.52$ MeV, $E_\nu = 10$ MeV, $|\vec{q}| = 5$ MeV), μ is Chemical Potential of Electrons

in respect to the variation of temperature for a certain range of energy transfer from neutrinos.

The differential cross-section of neutrino interactions with an electron at fixed temperature $T=40$ MeV, for the contribution of weak interaction, electromagnetic interaction, interference and the total of all the interactions, are shown in Fig. 2. For finite temperature ($T > 0$ MeV), there are several factors need to be considered, namely the retardation, Pauli blocking and detailed balance, because the effects are indeed quite significant. In the left panel of Fig. 2, the thick line shows the influence of retardation factor, the dotted line to show the influence of detailed balance factor and the dashed line shows the effect of Pauli blocking factor in the total cross-section.

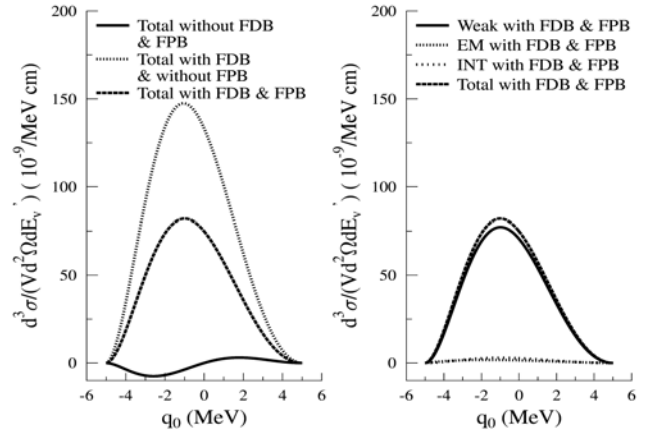


Figure 2. Comparison of Differential Cross-section of Weak Interaction, Electromagnetic Interaction, Interference and the Total for $T=40$ MeV ($\mu = 7.88$ MeV, $|\vec{q}| = 5$ MeV, $E_\nu = 10$ MeV, $R_\nu = 5 \times 10^{-6}$ MeV $^{-1}$, $\mu_\nu = 10^{-10}$ μ_B). FDB (Detailed Balance Factor), FPB (Pauli Blocking Factor)

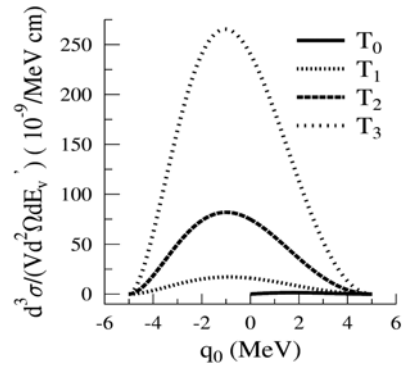


Figure 3. Comparison of the Total Differential Cross-section ($T_0 = 0$ MeV, $\mu_0 = 50$ MeV, $T_1 = 20$ MeV, $\mu_1 = 26.79$ MeV, $T_2 = 40$ MeV, $\mu_2 = 7.88$ MeV, $T_3 = 60$ MeV, $\mu_3 = 3.52$ MeV, $|\vec{q}| = 5$ MeV, $E_\nu = 10$ MeV, $R_\nu = 5 \times 10^{-6}$ MeV $^{-1}$, $\mu_\nu = 10^{-10}$ μ_B)

It is important to note here that the detailed balance factor raises the value of differential cross-section, but otherwise the Pauli blocking factors suppress the magnitude of differential cross-section. The total effect of these two factors is increasing the magnitude of the differential cross-section value. So if the temperature of the medium (electron matters) was raised, then the differential cross-section of neutrino-electron scattering in the medium was also increased. This finding can be understood because when the temperature was raised the electrons in the medium becomes more energetic, so that the possibility of interaction of neutrinos with electrons becoming more frequent. This will increase the magnitude of the cross-section because as already mentioned before the effect of detailed balance and Pauli blocking factors increase the cross-section. The significant increase in value of transverse and longitudinal polarization caused by increasing temperature is the reason. This can be also seen more clearly in Fig. 3 where the differential cross-section of neutrinos with electron matters for fixed density and various temperature are shown. While on the right panel of Fig. 2, it is shown the contribution of weak, electromagnetic interaction and interference. It can be seen obviously that for the corresponding value of the dipole moment of neutrinos and neutrino charge radius used in calculation, the weak interaction provides the dominant contribution. This fact is consistent with the standard model where the weak interaction dominated the neutrino interaction. But there are also other contributions, namely the electromagnetic interaction and interference, caused by the neutrino electromagnetic form factors, although the effect is not as strong as the weak interaction. This finding is also consistent with the obtained result using $T=0$ MeV approximation [6]. Note, for subsequent pictures, the total differential cross-section is presented by taking into account the retardation, Pauli blocking and detailed balance factors.

Before we go deeper into the effects of electromagnetic properties of neutrinos in warm and dense matter, as completeness in Fig. 4 is shown the variation of electron density on the cross-section of neutrino interactions with electrons at two fixed temperatures $T=20$ MeV and $T=60$ MeV. As we expected that the higher target density used, then the more frequent interaction of neutrinos with the target electrons. Consequently, the closer the constituents one to each other in the matter then the larger the cross-section. Of particular interest is at low temperature, the neutrino cross-section seems more controlled by the increase in pressure and electron density. But at high temperature, the neutrino cross section is more controlled by the temperature rise. So that it is evident in Fig. 4 that the effect of the variations of electron density is more significant at lower temperatures.

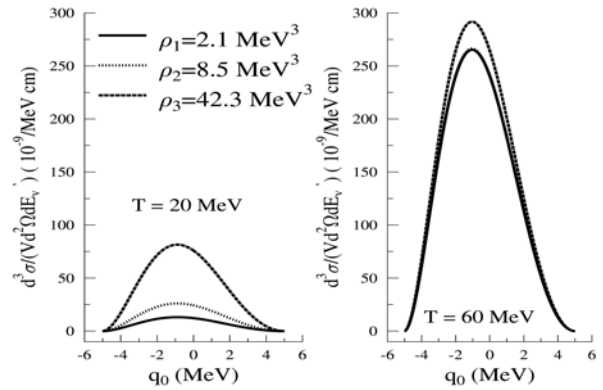


Figure 4. Comparison of the Cross-section with Variation of Electron Density ($|\vec{q}| = 5$ MeV, $E_\nu = 10$ MeV, $R_\nu = 5 \times 10^{-6}$ MeV, $\mu_\nu = 10^{-10} \mu_B$)

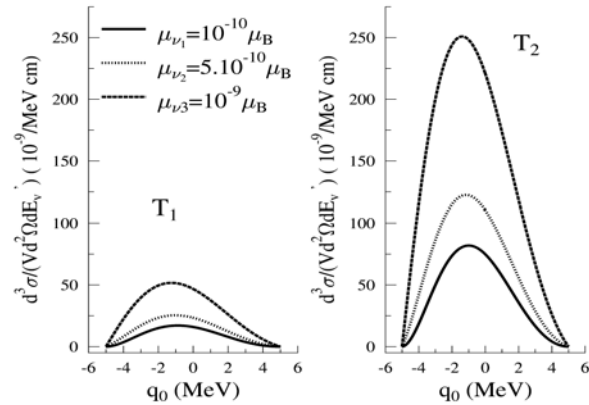


Figure 5. Comparison of Differential Cross-section with Variation of the Dipole Moment of the Neutrino ($T_1 = 20$ MeV, $\mu_1 = 26.79$ MeV, $T_2 = 40$ MeV, $\mu_2 = 77.88$ MeV, $|\vec{q}| = 5$ MeV, $E_\nu = 10$ MeV, $R_\nu = 5 \times 10^{-6}$ MeV $^{-1}$)

Fig. 5 shows the effect of variation of the dipole moment of neutrinos (μ_ν) with units of Bohr magneton (μ_B), for different temperatures of the cross-section of neutrinos. It can be seen that the effects of neutrino dipole moment become significant for both low and high temperature at $\mu_\nu \geq 5 \times 10^{-9} \mu_B$. This effect becomes more pronounced for high-temperature electron matters. This is quite consistent with the results of previous studies using $T=0$ MeV approximation [6-7].

Fig. 6 shows the influence of variations of the neutrino charge radius (R_ν) for different temperature of the cross-section of neutrinos. It is shown that in a reasonable range of R , the effect of the neutrino charge radius is not sufficiently visible, especially for relatively low temperature. The observed effect can only be seen when $T \geq 40$ MeV and $R_\nu \geq 5 \times 10^{-6}$ MeV $^{-1}$.

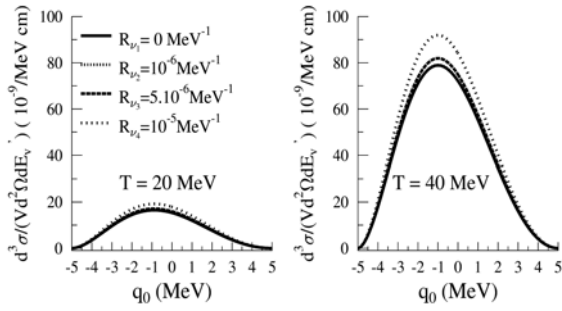


Figure 6. Comparison of Differential Cross-section with Variation of Temperature and Neutrino Charge Radius ($|\vec{q}|=5 \text{ MeV}$, $E_\nu=10 \text{ MeV}$, $\mu_\nu=10^{-10} \mu_B$)

After $\mu_\nu \geq 5 \times 10^{-9} \mu_B$ and $R_\nu \geq 5 \times 10^{-6} \text{ MeV}^{-1}$ neutrino electromagnetic contribution becomes more significant because the value of the sum of the longitudinal and transverse polarization, which is the most dominant component in the cross section for the electromagnetic contribution, rose significantly. The same reason is also found in the case of multi-component matter where the electrons are only part of them by using $T = 0 \text{ MeV}$ approximation [6-7].

RPA approach and the effective photon mass effect.

Effect of RPA correlation for the dense matter with $T = 0 \text{ MeV}$ and $T \neq 0 \text{ MeV}$ based on the standard model neutrino interactions with matter was investigated by the authors in Refs. [9,22]. The importance of this effect on the transport of neutrinos in supernova collapse and neutron star cooling was discussed [9,22]. But the calculation of neutrino transport in the matter by including electromagnetic properties of neutrinos and taking into account the RPA correlations at finite temperatures has not been done. Also effective photon mass effect (MPE) in the medium with varied density has not been investigated. Effective photon mass effects have been investigated to determine the neutrino mean free path in the case of supernova r-process nucleosynthesis [18] using constant density approximation. Therefore on this occasion the effect of RPA and MPE was studied, for the case where the electromagnetic properties of neutrinos are taken into account.

The left panel of Fig. 7 shows the RPA correlations which reduce the differential cross-section to about 20% compared to the cross section calculated by linear response approach for $T = 0 \text{ MeV}$ case, but the effect of MPE is not observed in this case. The right panel of Fig. 7, it is shown in the case $T = 10 \text{ MeV}$, the RPA correlations reduce the cross-section of nearly reached 80% compared to the cross section calculated with the linear response approach. In this case a small contribution of MPE appears to increase the cross-section, especially when the RPA is also taken into

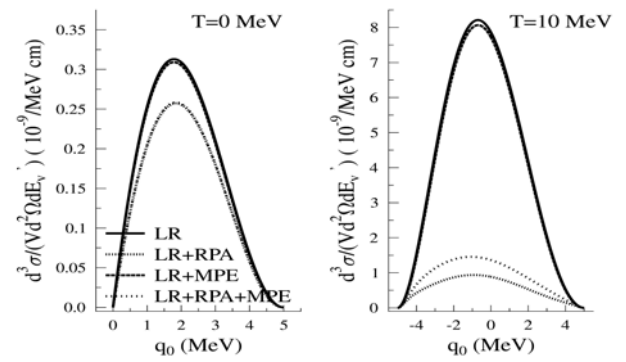


Figure 7. Comparison of Differential Cross-section for the Electron Density is Fixed for the Case Linear Response Approach, the RPA and MPE are Included for $E_\nu = 10 \text{ MeV}$, $R_\nu = 5 \times 10^{-6} \text{ MeV}^{-1}$ and $\mu_\nu = 10^{-10} \mu_B$

account. This means that the RPA correlations on the differential cross-section are very significant for finite temperature. While the influence of MPE is emerging for $T \geq 10 \text{ MeV}$ with condition that the RPA is also taken into account. In this calculation $R_\nu = 5 \times 10^{-6} \text{ MeV}^{-1}$ and $\mu_\nu = 10^{-10} \mu_B$ are used. The decrease in the cross-section of neutrinos due to the effects of RPA correlations can be understood because the correlations among the electrons cause the electrons become less energetic, especially at high temperature so that the probability of neutrino interactions with electrons is reduced. As the consequence, the cross-section becomes smaller. On the other hand, the damping effect on electromagnetic propagator in the RPA at high temperature due to MPE produces slightly reduction on the RPA contribution. This yields slightly value increase of the cross-section of neutrino.

4. Conclusion

The effects of neutrino electromagnetic form factors and the importance of the contribution of retardation, detailed balance and the Pauli blocking factors, for neutrino cross-section in dense matter and finite temperature are studied. The many-body effects on the target matter using a random phase approximation and the effective photon mass are also investigated. It is found that the effect of dipole moment is rather sensitive to the differential cross-section and the effect becomes greater when the matter temperature rises. Conversely differential cross-section is less sensitive to changes in the radius of the charged neutrino. The significant effects of the electromagnetic properties of neutrinos on cross-section emerge if the dipole moment of the neutrino $\mu_\nu \geq 5 \times 10^{-9} \mu_B$ and the charge radius of neutrinos $R_\nu \geq 5 \times 10^{-6} \text{ MeV}^{-1}$. Our finding is in agreement with ones that obtained in previous studies using zero temperature approximation. We have found also that the

detailed balance factor increase, while the Pauli blocking reduce the magnitude of the differential cross-section. The weak interaction provides the dominant contribution in cross-section. This finding is in consistent with the standard model. The contribution of electromagnetic interaction and interference can be ignored only to the extent that the dipole moment of neutrinos $\mu_\nu \leq 5 \times 10^{-9} \mu_B$ and neutrinos' charge radius of $R_\nu \leq 5 \times 10^{-6} \text{ MeV}^{-1}$. We have also found that the cross-section of neutrino interaction with matter is sensitive in respect to the temperature and density variations. For the later, it is pronounced especially at low temperature, while for the temperature variation case, in addition to detailed balance and the Pauli blocking factors, this effect is also influenced by the fact that the two most dominant polarizations, i.e. the longitudinal and transverse polarizations are very sensitive to temperature changes. Effect of the RPA correlations reduces the differential cross-section for zero and finite temperature. And the influence of MPE is quite marginal for both zero and finite temperatures when compared to one from the RPA, but with rising temperatures MPE effect little by little begin to emerge.

References

- [1] S. Reddy, M. Prakash, J.M. Lattimer, J.A. Pons, Phys. Rev. C 59 (1999) 2888.
- [2] M.T. Keil, Dissertation, Universitat Technischen Munchen, *arXiv: astro-ph.*, 2003, 0308228.
- [3] C. Giunti, W.K. Chung, Fundamentals of Neutrino Physics and Astrophysics, Oxford University Press, New York, 2007, p.180.
- [4] Z. Daraktchieva, J. Lamblin, O. Link, C. Amsler, M. Avenier, C. Broggin, J. Busto, C. Cerna, G. Gervasio, P. Jeanneret, G. Jonkmans, D.H. Koang, D. Lebrun, F. Ould-Saada, G. Puglierin, A. Stutz, A. Tadsen, J.L. Vuilleumier, Phys. Lett. B 564 (2003) 190.
- [5] E. Nardi, AIP. Con. Proc. 670 (2003) 118.
- [6] C.K. Williams, P.T.P. Hutaaruk, A. Sulaksono, T. Mart, Phys. Rev. D 71 (2005) 017303.
- [7] A. Sulaksono, C.K. Williams, P.T.P. Hutaaruk, T. Mart. Phys. Rev. C 73 (2006) 025803.
- [8] S. Reddy, M. Prakash, J.M. Lattimer, Phys. Rev. D 58 (1998) 013009.
- [9] C.J. Horowitz, K. Wehrberger, Phys. Lett. B 266 (1991) 236.
- [10] K. Saito, T. Maruyama, K. Soutome, Phys. Rev. C. 40 (1989) 407.
- [11] C. Giunti, A. Studenikin, Phys. Atomic Nucl. 72 (2009) 2089.
- [12] J. Barranco, O.G. Miranda, T.I. Rashba, Phys. Lett. B 662 (2008) 431.
- [13] W. Grimus, T. Schwetz, Nucl. Phys. B 587 (2000) 45.
- [14] A.B. Balantekin, C. Volpe, Phys. Rev. D 72 (2005) 033008.
- [15] J.F. Beacom, P. Vogel, Phys Rev. Lett. 83 (1999) 5222.
- [16] L. Satiawati, Thesis, University of Indonesia, Indonesia, 2011.
- [17] C.J. Horowitz, M.A. Perez Garcia, Phys. Rev. C 68 (2003) 025803.
- [18] A.B. Balantekin, C. Volpe, J. Welzel, JCAP. 0709 (2007) 016.
- [19] E. Braaten, D. Segel, Phys. Rev. D 48 (1993) 1478.
- [20] S. Reddy, M. Prakash, Astrophys. J. 478 (1996) 689.
- [21] K. Lim, C.J. Horowitz, Nucl. Phys. A 501 (1989) 729.
- [22] C.J. Horowitz, K. Wehrberger, Nucl. Phys. A 531 (1991) 665.